Performance Testing of a Piezoelectric Device for Extracting Energy from Vibrations

Giorgia Leonardi, Fabio Passacantilli, Carmen Galassi, and Daniele Dessi

Abstract Energy harvesting from ambient sources is an interesting opportunity for wireless and self-powered electronics, increasing research efforts toward the development of new devices. Among all energy sources, vibrations seem particularly convenient for this kind of application. Piezoelectric resonant systems, though offering configurations well suited to recover energy from vibrations, suffer from narrow operational bands, and for this reason new solution to enhance performances at off-design excitation conditions is sought. In this paper a piezoelectric resonant energy harvester is developed, focusing the attention on both ceramics production method and support material choice in order to maximize the oscillation amplitudes, and consequently the energy output. The device produced at ISTEC laboratories is then compared with a commercial product under harmonic excitations. Results relative to power output show that the in-house assembled device has better performance than the commercial one in the considered tested conditions, both in absolute terms and with respect to the active piezoelectric volume of the two devices.

1 Introduction

In recent years, the growing importance of wireless and off-grid devices has increased the interest on distributed power production even equipping the devices itself. In particular, ambient and anthropic vibrations are promising energy sources worth to be explored, driving the development and optimization of many new different devices. In literature, the usefulness of vibrations in powering wireless

G. Leonardi · D. Dessi (✉)
CNR-INM – National Research Council of Italy, Institute of Engineering for Sea, Roma (RM), Italy
e-mail: giorgia.leonardi@uniroma1.it; daniele.dessi@cnr.it

F. Passacantilli · C. Galassi
CNR-ISTEC – National Research Council of Italy, Institute of Science and Technology for Ceramics, Faenza (RA), Italy
e-mail: fabio.passacantilli@istec.cnr.it; carmen.galassi@istec.cnr.it

W. Zamboni, G. Petrone (eds.), *ELECTRIMACS 2019*, Lecture Notes in Electrical Engineering 615, https://doi.org/10.1007/978-3-030-37161-6_32

and low-consumption sensors for off-grid exercise has been shown in different applications, such as monitoring of civil structures [1], buildings [2], machineries [3], and human health [4, 5], where no from-grid power supply is possible or cabling would be too expensive and complicated.

In this kind of applications, one of the most effective systems is the piezoelectric resonant energy harvester in cantilevered configuration [6, 7]. However, even if the conversion efficiency at resonant frequency is high, the performance drops as soon as the devices is working out of its narrow resonance bandwidth. This behaviour makes the piezoelectric resonators difficult to be optimized for on-field applications, since ambient vibrations usually are not confined to a single frequency, and in reverse are stochastic with most of the energy spread over a large frequency range.

Many research groups worldwide are studying different technological solutions, trying to widen the acceptable frequency range and the overall energy conversion efficiency. A critical component for increasing global performances is provided by the electrical conversion system, that rectifies and stores the energy produced by the harvester to make it usable for electronic devices. Indeed, this element of the conversion chain can optimize the power output both searching for RC resonance conditions and using active circuit for conversion (MPPT, SSHI, SECE), as pointed out by Du et al. [8–10]. Furthermore, there are many techniques to improve the mechanical performance based on tuning with excitation frequencies and on increasing the oscillation amplitude with the same excitation input. The most widespread solution is inserting a tip mass to the cantilever end [11–13], changing the resonant frequency of the system and enhancing the amplitude of oscillations. Another technique consists in making the structure impact with an external element [14], such as a pendulum; in this way, the low-frequency vibrations can be transformed into higher frequency forces, more suitable to the typical cantilever mechanical configuration [15–17]. Moreover, in order to enhance amplitude oscillations, non-linearities in the resonant system can be introduced, for example, using a magnetic tip mass interacting with another magnet fixed out of the oscillator [12, 18–20], connecting several linear resonators to each other with springs [21, 22], using bistable or tristable configurations [22–25], or adopting support elements to piezoelectric materials with a snap-through behaviour [24, 26–28].

In this paper a vibration energy conversion system is presented and tested using a dedicated experimental setup, which simulates the vibrating support of the harvester. The piezoelectric production process, carried out at the ISTEC laboratory, is described and a new support material for the resonator is adopted. A comparison of the device with a commercial piezoelectric under sinusoidal signals is made, analysing performances in terms of power production.

2 Mechanical Configuration

The energy harvester adopted in this work exploits the direct piezoelectric effect via the use of a piezoelectric cantilever vibrating because of the basement excitation, as shown in Fig. 1

The piezoelectric material is known to couple the material stress $\boldsymbol{\sigma}$ and deformation $\boldsymbol{S}$ with the electric displacement $\boldsymbol{D}$ and field $\boldsymbol{E}$, according to the following state equations:

$$\begin{bmatrix} \boldsymbol{S} \\ \boldsymbol{D} \end{bmatrix} = \begin{bmatrix} \boldsymbol{c}^E & \boldsymbol{d}^t \\ \boldsymbol{d} & \boldsymbol{\varepsilon}^\sigma \end{bmatrix} \begin{bmatrix} \boldsymbol{\sigma} \\ \boldsymbol{E} \end{bmatrix}, \tag{1}$$

where $\boldsymbol{\varepsilon}$, $\boldsymbol{d}$, and $\boldsymbol{c}$ represent the electrical, piezoelectric, and elastic properties of the material, respectively. Equations (1) model the linear relation between deformation and charge, and describes both direct and converse effect. The direct effect (or generator behaviour) manifests when there is a charge production in the material after an imposed mechanical stress. On the contrary, the converse effect (or motor behaviour) occurs when a strain in the material is induced by an external electric field (or a voltage applied).

The mechanical configuration chosen for the device is the cantilevered one, with a clamped edge and the other free (Fig. 1); this appears the best layout to exploit ambient vibrations through piezoelectricity in terms of efficiency and simplicity. It is a common practice to glue the piezoelectric lamina over a supporting plate for several reasons: mechanical stability, structural integrity, ease of installation, and no charge compensation. In the present case, the support material is harmonic steel, which provides low-damping features. The support layer thickness has been chosen to contain the neutral axis of the overall structure (Fig. 2), since this allows the piezoelectric material to be more uniformly stretched or shorten through its thickness. Indeed, if the neutral axis be placed inside the piezoelectric sheet, the material would have a partial or even total charge cancellation, and so a decreased power output.

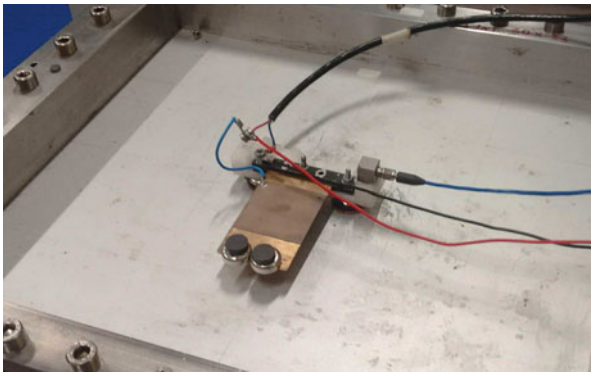

Fig. 1 Mechanical configuration of the piezoelectric harvester

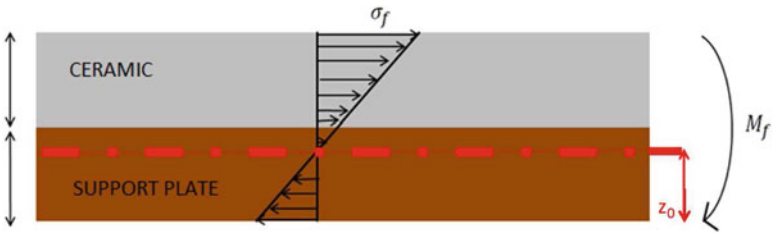

Fig. 2 Sketch of the optimal mechanical configuration

3 Piezoelectric Patch Production

In order to create a resonator well performing at low frequencies, the piezoelectric lamina was produced ad hoc at the CNR-ISTEC laboratory. The piezoelectric is produced with a tape casting process, particularly useful when a thin thickness (220 μm) needs to be reached. To create the ceramic material, a suspension based on the ceramic powder dispersed in an organic liquid with deflocculant, binder, and plasticizer is prepared [29]. The ceramic powder is lead-zirconate-titanate doped with niobium and lanthanum (PLZTN):

$$(Pb_{0.93}\ La_{0.07})\ [(Zr_{0.60}\ Ti_{0.40})_{0.9825}\ Nb_{0.0175}]\ O_3. \tag{2}$$

The additives are constituted by a dispersant, stabilizing colloidally the suspension and so avoiding agglomerates formation, a plasticizer, making tapes flexible and so possible to be bended, and a binder, binding together the particles. The solvent is an azeotropic mixture of methylethylketone (MEK) (or 2-butanone), 67% by weight, and ethanol (EtOH).

To level the thickness of the layers to 278 μm, the suspension moves on a belt and passes under a blade (Fig. 3). Then, after the drying process, the flexible solid tape can be punched or cut to obtain different shapes. Thus, the material obtained undergoes elimination of organic components (debonding) and sintering, and finally electrodes deposition by screen printing. At the end, the poling phase induces piezoelectric properties in the ferroelectric material, by orienting the electrical dipoles under a 3 kV/mm electrical field for 40 min in a silicon oil bath at 120 °C.

4 Conversion System

As the voltage output from the piezoelectric device is not constant, but varies in time due to the unsteady excitation, an electric conversion system is required to provide an output signal suitable to power an electronic device or to store temporarily the available energy. The system is schematically made of a voltage multiplier,

Fig. 3 Casting bench

acting also as rectifier, a charge regulator, and a capacity storage, which the load to be powered is attached to (Fig. 4). In the present case, the load is a temperature sensor. The voltage multiplier has six steps, each one made by Schottky BAT54CL diodes and tantalum capacitors of 4.7 μF, and it is able to multiply the input signal amplitude up to about six times. This circuital element makes possible for the piezoelectric harvester to reach the minimum threshold needed to activate the charge regulator BOB 09946. The output DC voltage from the BOB 09946 can take the values 1.8, 2.5, 3.3, and 3.6 V. Taking a closer look to the device, the LTC3588-1 integrated circuit (Fig. 5), optimized for high impedance devices as in piezoelectric applications, changes the input voltage into one of the aforementioned values thanks to a high efficiency buck converter. The UVLO component keeps the voltage off the buck converter until it reaches a threshold value, thanks to a capacitor optimized in order to lower the time needed to be charged. When the threshold is reached, the buck converter is activated, but it supplies voltage only when the load is connected at the output of the PLC and demands power.

Out of the BOB 09946, a capacitor (1500 μF) is used as storage to ensure a constant power flow for several seconds, enough in this case to perform a temperature measurement. The sensor indeed is activated thanks to an enable signal from BOB 09946 that controls a MOSFET: the circuit is closed only when the capacitor reaches 3.3 V and the sensor goes off when the voltage drops under 3 V. Figure 6 is a picture of piezoelectric harvester, conversion system, and temperature sensor.

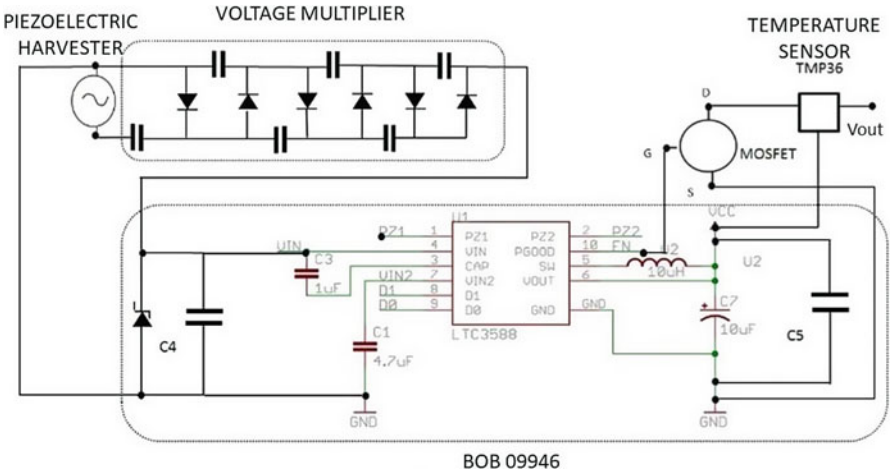

Fig. 4 Schematic representation of piezoelectric generator, conversion system, and temperature sensor

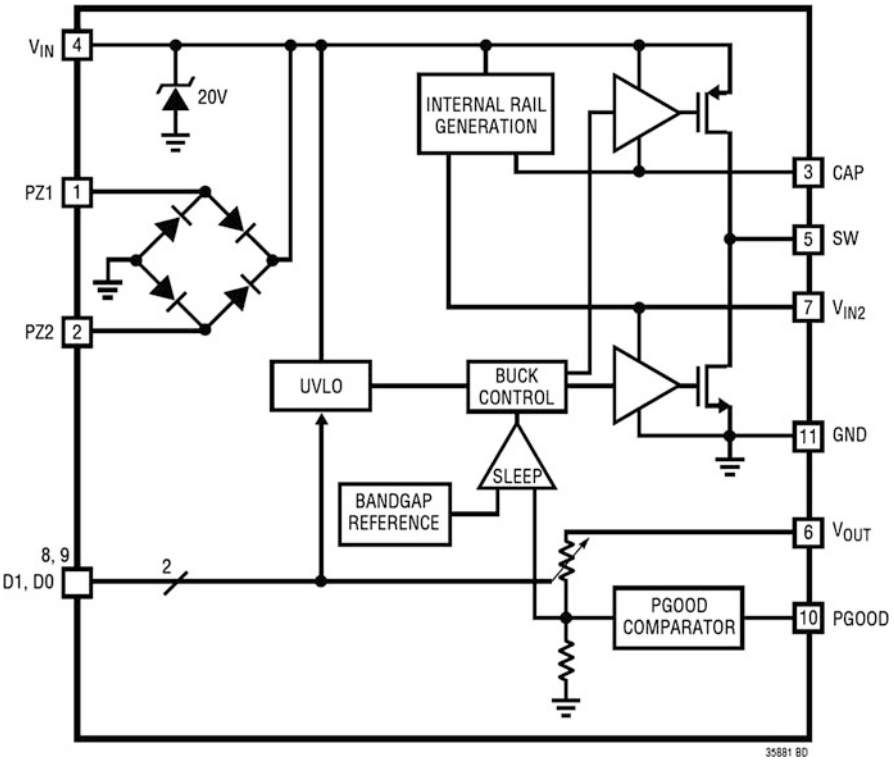

Fig. 5 Schematic representation of LTC3588-1

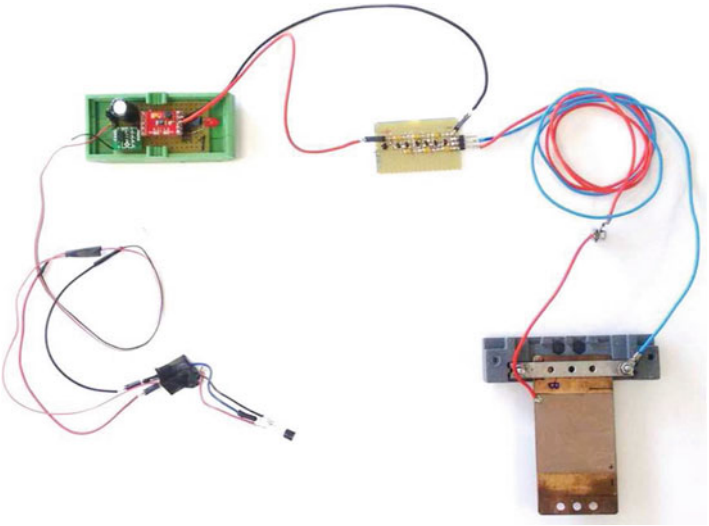

Fig. 6 Photo of piezoelectric harvester, conversion system, and temperature sensor

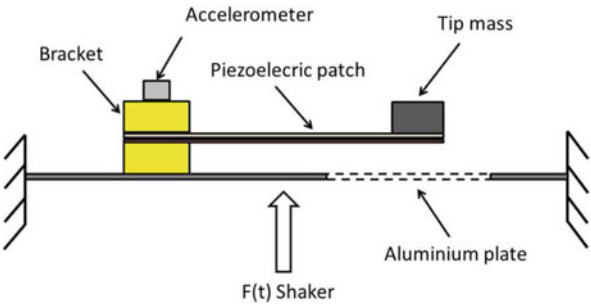

Fig. 7 Schematic configuration of the experimental setup

5 Experimental Setup

Assessing the performances of the harvester under variable conditions required to build an experimental setup made of several components, comprising a test-rig to host the vibrating plate, an excitation system via a shaker, and some sensors.

The energy harvester lies on a clamped metallic plate, simulating a real-life installation (e.g. wall or floor), excited by a force applied with the shaker (Fig. 7). The LMS acquisition system collects the signals provided by an accelerometer, placed at the clamping of the piezoelectric device, and a voltage meter between the piezoelectric electrodes. To ensure that the devices are tested under the same excitation, the accelerometer measurement is taken as reference, because though applying the same force the different mass of the devices may significantly alter the overall response. For this purpose, a reverse engineering process allows us to find which force signal must be set to obtain the desired acceleration. This can be done by

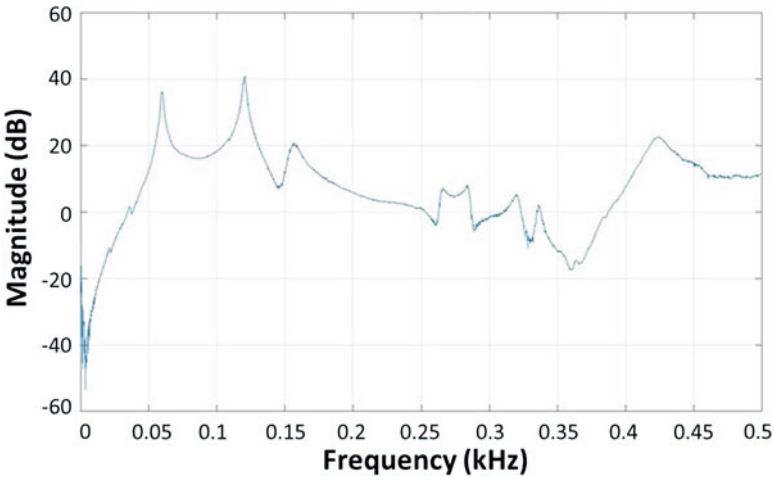

Fig. 8 Frequency transfer function of the plate

Table 1 Voltage output (rms) at $f_e = 56.6$ Hz harmonic excitation

Device	Voltage output	Output/input ratio
In-house assembled	9.23 V	3.69 V·s^2/m
Commercial	7.30 V	2.92 V·s^2/m

a trial-and-error procedure or with a general procedure that requires the calculation of the frequency transfer function (Fig. 8) between applied force and acceleration.

6 Results and Discussion

In this section the comparison between the in-house assembled device, also denoted in the following as ISTEC-S, and the commercial product (MIDE PPA 1012) will be carried out to underline the main differences in performance between the two solutions.

The first test has been performed with a harmonic seismic excitation at an rms acceleration amplitude and frequency equal to 0.1 m/s^2 and 56.6 Hz, respectively, the latter being the resonance frequency of the ISTEC-S. To bring the resonance frequency of the MIDE PPA 1012 to the same value of 56.6 Hz, a tip mass has been added. Though this feature should favour the commercial solution, the rms voltage output, in open circuit conditions, of the ISTEC-S is 9.23 V, higher than 7.3 V of PPA 1012, as shown in Table 1.

The sensitivity of the two devices to perturbation of the optimal excitation frequency has been tested too. Both ISTEC-S and PPA 1012 have been equipped with a tip mass to lower their natural frequency f_n to 20 Hz (Fig. 9). Thus, five tests with sinusoidal excitation have been carried out at the same amplitude (0.6 m/s^2

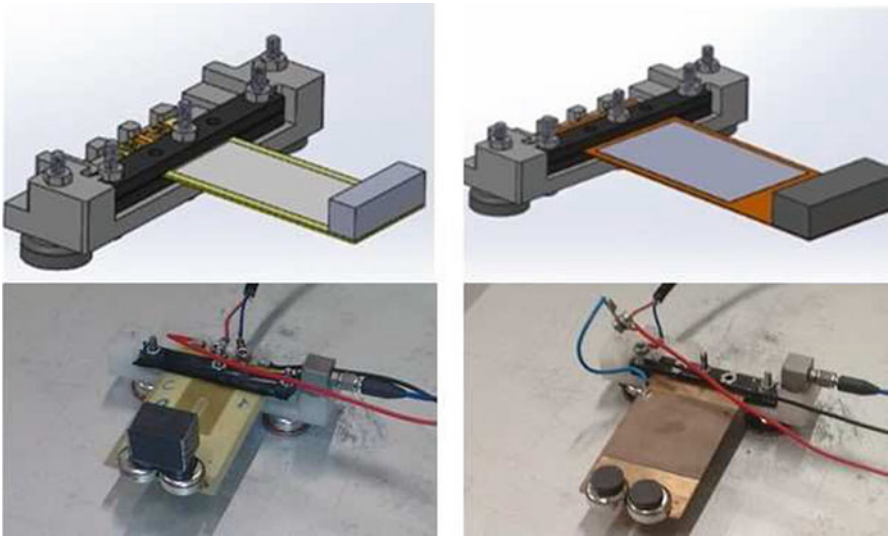

Fig. 9 Schematic and real configuration of the commercial (on the left) and the in-house assembled devices (on the right)

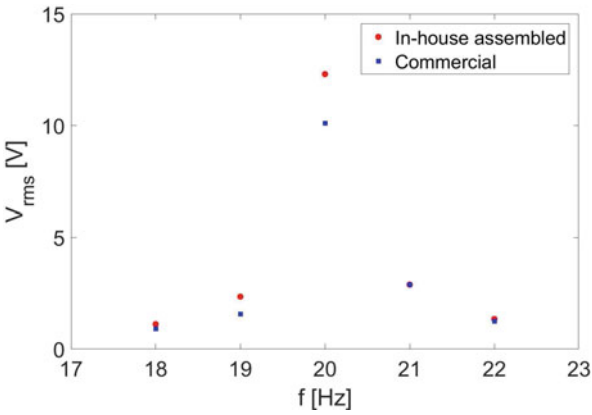

Fig. 10 Comparison between the commercial and in-house assembled devices output voltage for harmonic excitation at different frequencies

of rms), varying the excitation frequency f_e of $\pm 5\%$ and $\pm 10\%$ with respect to the initial value f_n. Results in Fig. 10 show the expected drop of performance for both devices out of the resonant frequency $f_e \neq f_n$. Anyway, ISTEC-S still provides a better performance at the resonant excitation and for $f_e > f_n$, through this difference becomes negligible for $f_e < f_n$.

In order to operate an absolute and a relative comparison between the two devices, the dimensions of the active piezoelectric materials have been reported in Table 2. Both devices have been tested for different resistive loads, varying from 0.82 kΩ till 90 kΩ (Figs. 11 and 12). The curves show an optimal load condition

Table 2 Dimensions of the active piezoelectric material

Device	L×W×T [mm]	Area	Volume
In-house	40×40×0.2	1600 mm^2	320 mm^3
Commercial	46×38.4×0.25	1766 mm^2	442 mm^3

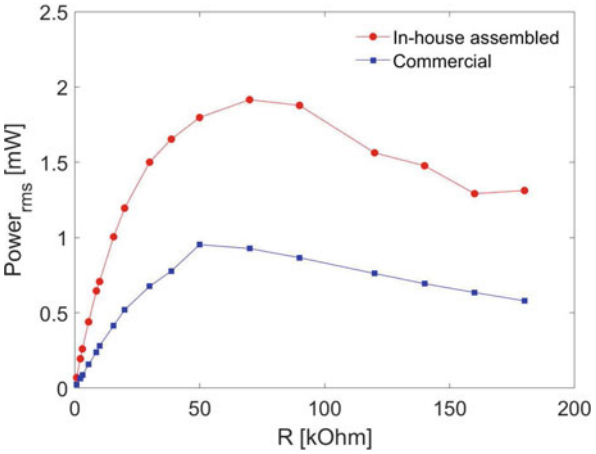

Fig. 11 Comparison between the power output of the in-house and the commercial devices for different resistive loads

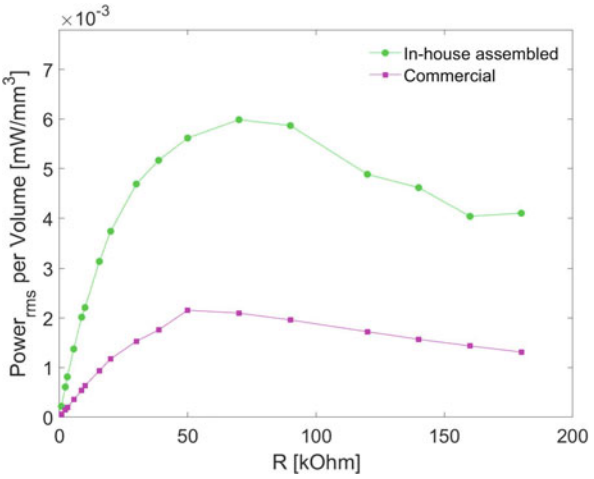

Fig. 12 Comparison between the power output per volume of the in-house and the commercial devices for different resistive loads

at 70 kΩ for the ISTEC-S device and at 50 kΩ for the PPA 1012, as suggested by the analysis of the equivalent RC circuit describing the system. Both power output and power per volume of active piezoelectric material results point out a better performance of the ISTEC-S with respect to the commercial solution.

At the end, the performances of the two devices are experimentally compared considering their response in a realistic working case, where the load is given by a resistive temperature sensor (TMP36 by Analog Devices). The test has been carried out with a harmonic seismic excitation at an rms acceleration amplitude and frequency equal to 0.1 m/s^2 and 20 Hz, respectively. The initial charge of the storage

Table 3 Recharge times of the storage capacitor

Device	First charge time	Temperature data sample time
In-house	5 min	27 s
Commercial	9 min	48 s

capacity takes a longer time than intermediate charging between sensor recordings (see Table 3), as the 3.3 V threshold has to be reached from scratch. Indeed, the intermediate charges are operated in a shorter period, since the MOSFET of the sensor opens only when the voltage drops from 3.3 to 3 V, and the capacity voltage has to rise of just 0.3 V. Both devices power successfully the load, but recharge time is 27 s for ISTEC-S against 48 s of PPA 1012, as shown in Table 3.

7 Conclusions

In this work, a piezoelectric device for recovering energy from vibrations has been tested up to verify its capability to provide enough power to measure ambient temperature within acceptable vibration levels; under harmonic excitation of 20 Hz, the whole-body 1-h exposure limit is about 10 m/s^2 according to ISO 2631, far higher than test excitation. Keeping the same cantilever configuration, the performance assessment of two different layouts in terms of materials and geometries (one built at CNR-ISTEC laboratory, the other fabricated by MIDE) has been carried out showing a larger voltage and power output for the in-house assembled device in the considered testing conditions both in absolute and relative to piezoelectric volume terms. Since one of the critical points is the tuning between the excitation and natural frequency of the cantilever, off-design excitation conditions have been tested highlighting the expected decrease of performances. On this aspect, there is the need to address more systematically off-design conditions by identifying both the acceptable operational envelope above the minimum power requirement of the sensor and the countermeasures to expand the operational margins.

Acknowledgements We wish to thank Carlo Baldisserri, Claudio Capiani, and Davide Gardini for their contribution in fabrication of ISTEC-S piezoelectric device and testing and Massimo Adriano for his support in setting the electronic components.

References

1. H. Wang, A. Jasim, X. Chen, Energy harvesting technologies in roadway and bridge for different applications—a comprehensive review. Appl. Energy. **212**, 1083–1094 (2018)
2. X.D. Xie, Q. Wang, Design of a piezoelectric harvester fixed under the roof of a high-rise building. Eng. Struct. **117**, 1–9 (2016)

3. B.C. Essink, R.B. Owen, D.J. Inman, Optimization of a zigzag shaped energy harvester for wireless sensing applications. Spec. Top. Struct. Dyn. **6**, 85–89 (2017)
4. M.T. Todaro, F. Guido, L. Algieri, V.M. Mastronardi, D. Desmaële, G. Epifani, M. De Vittorio, Biocompatible, flexible, and compliant energy harvesters based on piezoelectric thin films. IEEE Trans. Nanotech. **17**(2), 220–230 (2018)
5. N. Jackson, O.Z. Olszewski, C. O'Murchu, A. Mathewson, Shock-induced aluminium nitride based MEMS energy harvester to power a leadless pacemaker. Sensors Actuators A: Phys. **264**, 212–218 (2017)
6. Y. Kuang, M. Zhu, Characterisation of a knee-joint energy harvester powering a wireless communication sensing node. Smart Mater. Struct. **25**(5), 055013 (2016)
7. A.E. Kubba, K. Jiang, Efficiency enhancement of a cantilever-based vibration energy harvester. Sensors 2014 **14**, 188–211 (2013)
8. S. Du, Y. Jia, C.D. Do, A.A. Seshia, An efficient SSHI interface with increased input range for piezoelectric energy harvesting under variable conditions. IEEE J. Solid-State Circuits **51**(11), 2729–2742 (2016)
9. S. Du, A.A. Seshia, An inductorless bias-flip rectifier for piezoelectric energy harvesting. IEEE J. Solid-State Circuits **52**(10), 2746–2757 (2017)
10. S. Du, G.A. Amaratunga, A.A. Seshia, A cold-startup SSHI rectifier for piezoelectric energy harvesters with increased open-circuit voltage. IEEE Trans. Power Electron. **34**, 263–274 (2018)
11. N. Jackson, F. Stam, O.Z. Olszewski, R. Houlihan, A. Mathewson, Broadening the bandwidth of piezoelectric energy harvesters using liquid filled mass. Proc. Eng. **120**, 328–332 (2015)
12. Z. Hu, J. Qiu, X. Wang, Y. Gao, X. Liu, Q. Chang, Y. Long, X. He, An integrated multi-source energy harvester on vibration and magnetic field energy. AIP Adv. **8**(5), 2158–3226 (2018)
13. Y. Jia, A.A. Seshia, Power optimization by mass tuning for MEMS piezoelectric cantilever vibration energy harvesting. J. Microelectromechanical Syst. **25**(1), 108–117 (2016)
14. A. Abedini, S. Onsorynezhad, F. Wang, Study of an impact driven frequency up-conversion piezoelectric harvester, in *ASME 2017 Dynamic Systems and Control Conference, American Society of Mechanical Engineers*, pp. V003T41A005–V003T41A005 (2017)
15. D.M. Toma, M. Carbonell Ventura, D. Pujol Bresco, A. Manuel Lázaro, J. Miquel Masalles, An impacting energy harvester through piezoelectric device for oscillating water flow, in *MARTECH: 5th International Workshop on Marine Technology: 19th–20th of November*, Vilanova i la Geltrú, pp. 39–42 (2013)
16. N. Okada, S. Yabe, H. Fujimoto, M. Murai, Experiments on floating wave-power generation using piezoelectric elements and pendulums in the water tank, in *2012 Oceans-Yeosu, IEEE*, pp. 1–8 (2012)
17. C. Viñolo, D. Toma, A. Mànuel, J. del Rio, An ocean kinetic energy converter for low-power applications using piezoelectric disk elements. Eur. Phys. J. Spec. Top. **222**(7), 1685–1698 (2013)
18. A.M. Wickenheiser, Broadband and low frequency vibration-based energy harvesting improvement through magnetically induced frequency up-conversion, in *ASME 2010 Conference on Smart Materials, Adaptive Structures and Intelligent Systems, American Society of Mechanical Engineers*, pp. 611–618 (2010)
19. F. Cottone, H. Vocca, L. Gammaitoni, Nonlinear energy harvesting. Phys. Rev. Lett. **102**(8), 080601 (2009)
20. S. Zhou, J. Cao, D.J. Inman, J. Lin, S. Liu, Z. Wang, Broadband tristable energy harvester: modelling and experiment verification. Appl. Energy **133**, 33–39 (2014)
21. S. Zhou, D.J. Inman, J. Cao, A linear-element coupled nonlinear energy harvesting system, in *ASME 2015 Conference on Smart Materials, Adaptive Structures and Intelligent Systems, American Society of Mechanical Engineers*, pp. V002T07A007–V002T07A007 (2015)
22. S. Zhou, J. Cao, D.J. Inman, S. Liu, W. Wang, J. Lin, Impact-induced high-energy orbits of nonlinear energy harvesters. Appl. Phys. Lett. **106**(9), 093901 (2015)
23. J. Cao, A. Syta, G. Litak, S. Zhou, D.J. Inman, Y. Chen, Regular and chaotic vibration in a piezoelectric energy harvester with fractional damping. Eur. Phys. J. Plus **130**(6), 103 (2015)

24. S.A. Emam, J. Hobeck, D.J. Inman, Experimental study of nonlinear vibration energy harvesting of a bistable composite laminate, in *Proceedings of the ASME 2017 Conference on Smart Materials, Adaptive Structures and Intelligent Systems* (2017)
25. W. Wang, J. Cao, C.R. Bowen, D.J. Inman, J. Lin, Performance enhancement of nonlinear asymmetric bistable energy harvesting from harmonic, random and human motion excitations. Appl. Phys. Lett. **112**(21), 213903 (2018)
26. D.N. Betts, C.R. Bowen, H.A. Kim, N. Gathercole, C.T. Clarke, D.J. Inman, Nonlinear dynamics of a bistable piezoelectric-composite energy harvester for broadband application. Eur. Phys. J. Spec. Top. **222**(7), 1553–1562 (2013)
27. T.S. Mehdi, An analytical study on piezoelectric-bistable laminates with arbitrary shapes for energy harvesting, in *7th ECCOMAS Thematic Conference on Smart Structures and Materials* (2015)
28. A.J. Lee, D.J. Inman, A multifunctional bistable laminate: Snap-through morphing enabled by broadband energy harvesting. J. Intell. Mater. Syst. Struct. (2018). https://doi.org/10.1177/1045389X18770895
29. D. Gardini, M. Deluca, M. Nagliati, C. Galassi, Flow properties of PLZTN aqueous suspensions for tape casting. Ceram. Int. **36**(5), 1687–1696 (2010)